Journal of Intelligent and Connected Vehicles
2023, **6**(3): 161–172
https://doi.org/10.26599/JICV.2023.9210016

Research Article

Vehicle sideslip trajectory prediction based on time-series analysis and multi-physical model fusion

Lipeng Cao[1,2], Yugong Luo[2], Yongsheng Wang[2], Jian Chen[2], Yansong He[1,✉]

[1]*College of Mechanical and Vehicle Engineering, Chongqing University, Chongqing 400030, China*
[2]*School of Vehicle and Mobility, Tsinghua University, Beijing 100084, China*

Received: April 17, 2023; Revised: June 16, 2023; Accepted: July 30, 2023

ABSTRACT: On highways, vehicles that swerve out of their lane due to sideslip can pose a serious threat to the safety of autonomous vehicles. To ensure their safety, predicting the sideslip trajectories of such vehicles is crucial. However, the scarcity of data on vehicle sideslip scenarios makes it challenging to apply data-driven methods for prediction. Hence, this study uses a physical model-based approach to predict vehicle sideslip trajectories. Nevertheless, the traditional physical model-based method relies on constant input assumption, making its long-term prediction accuracy poor. To address this challenge, this study presents the time-series analysis and interacting multiple model-based (IMM) sideslip trajectory prediction (TSIMMSTP) method, which encompasses time-series analysis and multi-physical model fusion, for the prediction of vehicle sideslip trajectories. Firstly, we use the proposed adaptive quadratic exponential smoothing method with damping (AQESD) in the time-series analysis module to predict the input state sequence required by kinematic models. Then, we employ an IMM approach to fuse the prediction results of various physical models. The implementation of these two methods allows us to significantly enhance the long-term predictive accuracy and reduce the uncertainty of sideslip trajectories. The proposed method is evaluated through numerical simulations in vehicle sideslip scenarios, and the results clearly demonstrate that it improves the long-term prediction accuracy and reduces the uncertainty compared to other model-based methods.

KEYWORDS: autonomous vehicle, sideslip trajectory prediction, adaptive quadratic exponential smoothing with damping (AQESD), interacting multiple model (IMM)

1 Introduction

When driving on a slippery highway, a vehicle may experience a sideslip due to the lateral force acting upon it exceeding the adhesion offered by the road surface. This phenomenon may cause the vehicle to drift out of its intended lane, thereby jeopardizing the safety of other vehicles on the road. Therefore, self-driving cars must be equipped with the ability to predict the future trajectory (Eskandarian et al., 2021) of sideslip vehicles around them to avoid collisions and ensure safety.

In the context of regular driving vehicles, drivers can exert normal control over the cars while adhering to traffic regulations. There are commonalities in the driving behaviors of different vehicles. Therefore, driving behavior patterns of vehicles on highways can be summarized from a large amount of naturalistic driving data. For example, the lane-changing behavior of vehicles can be modeled using a fifth-degree polynomial or trigonometric functions, while the car-following behavior can be modeled using a first-order Wiener process (Ghorai et al., 2022; Huang et al., 2022). By establishing the kinematic and behavioral models of vehicles, it is possible to predict their long-term trajectories with relatively high accuracy. However, when it comes to sliding vehicles, drivers are unable to effectively control them, and their trajectories no longer conform to traffic rules. This increases the randomness of the sliding vehicle trajectories, making it difficult to summarize their sliding behaviors using a mathematical model.

Moreover, with the advancement of deep learning techniques and the availability of large-scale naturalistic driving datasets, data-driven approaches can also be used to accurately predict the long-term trajectories of normally operating vehicles. However, there is currently a lack of datasets specifically focused on sliding vehicle trajectories. In the absence of sufficient data, deep learning methods cannot fully capture all the features of sliding trajectories, making it challenging to use a data-driven approach for accurate long-term prediction of sliding vehicle trajectories.

Given the aforementioned differences, the methods currently used for general trajectory prediction are not suitable for predicting sliding trajectories. Despite the differences between sliding and general trajectories, they both adhere to the vehicle's kinematic model. Therefore, the kinematic model can be utilized to predict the sliding trajectories of vehicles. However, the simple structure and constant input assumption of the vehicle kinematic model limit its accuracy to short-term trajectory prediction, rendering it unsuitable for long-term prediction (Ammoun and Nashashibi, 2009; Schubert et al., 2008).

In order to address the limitations of physical model-based methods, which often rely on the assumption of constant inputs that limit long-term prediction accuracy, this study proposes a novel method called time-series analysis and interacting multiple model-based (IMM) sideslip trajectory prediction (TSIMMSTP)

✉ Corresponding author.
E-mail: hys68@cqu.edu.cn

for predicting vehicle sideslip trajectories. The proposed method utilizes time-series analysis and multi-physical model fusion to achieve long-term and high-precision prediction. The overall architecture of the method is shown in Fig. 1. The time-series analysis module utilizes the adaptive quadratic exponential smoothing with damping (AQESD) to online learn the historical state sequence (e.g., acceleration, angular velocity) of the sideslip vehicle, capture its motion characteristics, and predict its future state sequence for input to the physical model. Considering that the driver cannot fully control the vehicle during sideslip, the interaction characteristics of the sideslip trajectory are weak, and hence this module does not need to capture the interactive characteristics of sideslip vehicles. In the sideslip trajectory prediction fusion module, the IMM is adopted to fuse the sideslip trajectory prediction results of multiple physical models according to the uncertainty of each physical model prediction result.

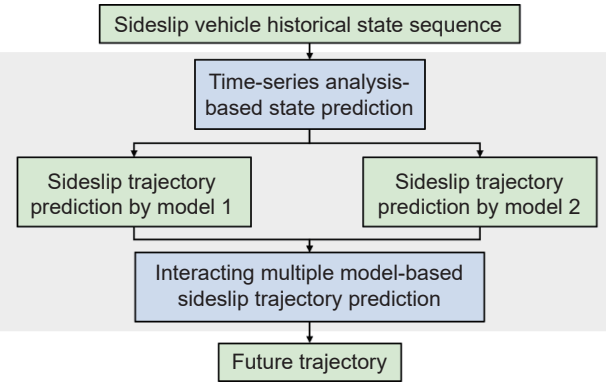

Fig. 1 Architecture of vehicle sideslip trajectory prediction based on time-series analysis and multi-physical model fusion.

Compared to physical model-based methods, the introduction of the time-series analysis module enables the physical model to achieve long-term and high-precision prediction of the sideslip trajectory. Furthermore, the introduction of the sideslip trajectory prediction fusion module improves the accuracy of the sideslip trajectory prediction and reduces the prediction uncertainty. The main contributions of this paper are two-fold:

1) The TSIMMSTP sideslip trajectory prediction method is proposed. The assumption of constant inputs in the physical model leads to a decrease in the long-term prediction accuracy. To address this issue, a time-series analysis module is designed to predict the inputs of the physical model, thereby improving its long-term prediction accuracy. Additionally, a single physical model is inadequate to capture the characteristics of vehicle sliding motion. Hence, the Interacting Multiple Model (IMM) approach is employed to fuse multiple physical models, reducing the uncertainty in sliding trajectory prediction.

2) A novel quadratic exponential smoothing method called AQESD is proposed for vehicle sideslip conditions. Traditional QES methods are prone to over-prediction, leading to deteriorated prediction results of the physical model. To address this issue, we introduce damping coefficients in the QES and design an adaptive computation method for damping coefficients and smoothing coefficients based on the final state estimation. This allows the time-series analysis module to provide more accurate input state sequences for the physical model, thereby improving the prediction accuracy of the physical model for sliding trajectories.

The structure of this paper is as follows. Section 2 provides a literature review of model-based and deep learning-based trajectory prediction. Section 3 introduces the proposed method and its related techniques. In Section 4, the application of the method is described, and the results are discussed. Finally, Section 5 concludes this paper.

2 Related works

This section presents a brief overview of the existing research on trajectory prediction, including both model-based and data-driven approaches. For a more comprehensive review of these research areas, please refer to the references listed in Gulzar et al. (2021) and Mozaffari et al. (2022).

Model-based trajectory prediction methods have gained significant attention from researchers due to their flexibility, reliability, and interpretability. In their work, Ammoun et al. (2009) proposed a Kalman filter-based trajectory prediction method that uses information from GPS and communication devices to assess the collision risk of vehicles. Another model-based approach for vehicle trajectory prediction was proposed by Park et al. (2015), which utilizes the Rapidly-Exploring Random Tree (RRT) with Gaussian Mixture Model (GMM) method for stereo camera systems. Kim et al. (2018) proposed a trajectory prediction method based on cross-swing angular acceleration and multi-rate Kalman filter to improve the control performance of adaptive cruise control (ACC). It is worth noting that these methods are designed for in-vehicle sensor systems. On the other hand, other scholars have proposed more general trajectory prediction methods by incorporating multi-model fusion techniques. For instance, Xie et al. (2017) and Houenou et al. (2013) proposed a fusion of physical and behavioral model prediction results to improve the long-term prediction performance of physical model-based trajectory prediction methods. Similarly, Wissing et al. (2018) proposed a model-based trajectory prediction method that incorporates behavioral classification and temporal probability estimation. Finally, to enable autonomous vehicles to predict the trajectory of other vehicles in any environment, Schreier et al. (2016) proposed a fused long-term trajectory prediction method that considers all vehicle behavioral and motion uncertainties.

The aforementioned studies have focused on improving trajectory prediction accuracy through the fusion of physical models with other models. However, they do not incorporate historical vehicle information into the physical model to enhance the accuracy of physical model prediction results.

Deep learning-based trajectory prediction methods have gained popularity due to their ability to model interactions between vehicles and incorporate vehicle history information. Alahi et al. (2016) used social pooling and Long Short-Term Memory (LSTM) neural networks for pedestrian trajectory prediction, while Deo et al. (2018) improved social pooling using convolution for vehicle trajectory prediction. Messaoud et al. (2019, 2021) have proposed methods that simulate interactions between neighboring vehicles for trajectory prediction, including non-local social pooling-based and attention mechanism-based approaches. Izquierdo et al. (2023) proposed a method that utilizes a bird's-eye view and convolutional neural networks (CNNs) for predicting vehicle trajectories in highway scenarios. To facilitate the development of low-cost connected automated vehicle systems, Yao et al. (2022) proposed the use of piecewise Taylor series approximation and piecewise Fourier series approximation techniques to reduce computational complexity, minimize device investment, and lower computational energy consumption. Other studies focus on the integration of physical constraints, traffic

rules, and environmental maps into deep learning-based trajectory prediction models. For example, Lane Graph Convolutional Network (LaneGCN) was proposed to capture complex topologies and dependencies of lane graphs (Liang et al., 2020), Trajectory Proposal Network (TPNet) was proposed to integrate physical constraints into data-driven trajectory prediction methods (Fang et al., 2020), and Prediction with Model-based Planning (PRIME) (Song et al., 2022) was proposed to generate accurate and feasible predictions of future trajectories (Song et al., 2022). Yao et al. (2023) proposed a physics-aware learning model for trajectory prediction in congested traffic scenarios within the context of vehicular networks.

Although deep learning-based trajectory prediction methods have shown promising results in improving prediction accuracy, recent studies have pointed out their limitations. According to Zhang et al. (2022), adversarial prediction can result in an increase in prediction error by more than 150% in deep learning-based methods. Similarly, Bahari et al. (2022) discovered that deep learning-based methods are prone to prediction failures when there is a change in the predicted scenario or insufficient data. These findings suggest that the deep learning-based approach still suffers from shortcomings in adversarial robustness and scenario generalization. The sideslip scenario in vehicles is a rare scenario with limited data, making it challenging to predict the trajectory of the vehicle using existing deep learning-based methods. While physical model-based methods can be adapted to the sideslip scenario, they do not consider the historical motion information of the vehicle, resulting in poor long-term prediction accuracy. To address this issue, this study proposes a vehicle sideslip trajectory prediction method that utilizes time-series analysis and multi-physics model fusion. Firstly, the historical information is incorporated into multiple physical models using quadratic adaptive exponential smoothing with damping, thereby improving the trajectory prediction accuracy. Next, the trajectory prediction results are fused using IMM to further enhance the prediction accuracy. This method effectively overcomes the issue of poor prediction accuracy of physical models for long time in the vehicle sideslip scenario.

3 Methods

In this paper, several coordinate systems are utilized and defined in this section, which is illustrated in Fig. 2. The global coordinate system with a fixed origin is referred to as the world frame and denoted as $\boldsymbol{G}$. The ego coordinate system is located at the geometric center of the ego vehicle and aligned with its velocity vector. It is represented by $\boldsymbol{L}$ and highlighted in orange in Fig. 2. The red vehicle denotes the ego vehicle, while the green one represents the observed sideslip vehicle.

This section presents the proposed vehicle sideslip trajectory prediction method architecture, including time-series analysis-based state prediction, physical model-based trajectory prediction, and IMM-based trajectory fusion. The assumption is made that the self-driving car is equipped with a target detection and tracking module and a high-precision map, which can observe the motion states such as position, attitude, speed, rotation rate, and acceleration of surrounding vehicles. The observed historical motion state information will be stored in the onboard computer for time-series analysis. It should be noted that this study focuses on the prediction method of sideslip trajectories, and the identification of sideslip behavior can be found in Xiang et al. (2022).

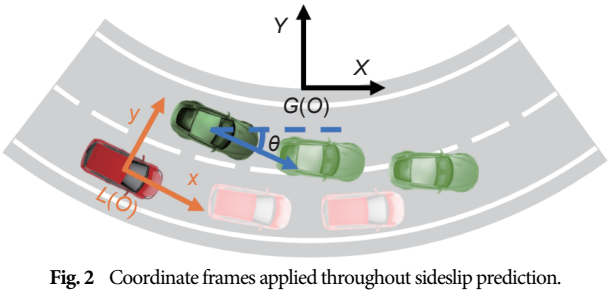

Fig. 2 Coordinate frames applied throughout sideslip prediction.

3.1 Physical model-based trajectory prediction

3.1.1 Vehicle kinematic model

The constant turning and acceleration (CTRA) and the constant acceleration (CA) models are selected, corresponding to model 1 and model 2 in Fig. 2, for predicting the sideslip trajectory. The state space of the CTRA model can be expanded as Eq. (1):

$$\boldsymbol{X}^1 = \begin{pmatrix} x & y & v & \theta & w & a \end{pmatrix}^T \tag{1}$$

where $\boldsymbol{X}^1$ is the state space vector of the CTRA model. (x, y) is the position and θ is the rotation angle of the observed vehicle in the global coordinate system. The variables w, v, and a represent the angular velocity, velocity, and acceleration of the observed vehicle in the ego coordinate system, respectively. The superscript ^{T} stands for transpose.

The discrete state transfer equation of the CTRA model (Schubert et al., 2008) can be formulated as Eq. (2):

$$\boldsymbol{X}^1_{k+1} = \boldsymbol{X}^1_k + \Delta\boldsymbol{X}^1_{k+1} \tag{2}$$

with

$$\boldsymbol{X}^1_{k+1} = \begin{pmatrix} \frac{1}{w^2}\left(-wv\sin(\theta) - a\cos(\theta) + a\cos(T_s w + \theta) + (T_s wa + wv)\sin(T_s w + \theta)\right) \\ \frac{1}{w^2}\left(wv\cos(\theta) - a\sin(\theta) + a\sin(T_s w + \theta) + (-T_s wa - wv)\cos(T_s w + \theta)\right) \\ T_s w \\ T_s a \\ 0 \\ 0 \end{pmatrix},$$

where T_s is the sampling interval time and k is the time step, in this study $T_s = 0.1$ s.

The state space of the CA model can be expanded as Eq. (3):

$$\boldsymbol{X}^2 = \begin{pmatrix} x & y & v_x & v_y & a_x & a_y \end{pmatrix}^T \tag{3}$$

where $\boldsymbol{X}^2$ is the state space vector of the CA model. v_x and a_x are the velocity and acceleration of the observed vehicle in the x-direction at the global coordinate, and v_y and a_y are the velocity and acceleration of the observed vehicle in the y-direction at the global coordinate, respectively.

The discrete state transfer equation of the CA model (Schubert et al., 2008) can be formulated as Eq. (4):

$$\boldsymbol{X}^2_{k+1} = \boldsymbol{A}\boldsymbol{X}^2_k \tag{4}$$

$$\text{with } \boldsymbol{A} = \begin{pmatrix} 1 & 0 & T_s & 0 & 0.5T_s^2 & 0 \\ 0 & 1 & 0 & T_s & 0 & 0.5T_s^2 \\ 0 & 0 & 1 & 0 & T_s & 0 \\ 0 & 0 & 0 & 1 & 0 & T_s \\ 0 & 0 & 0 & 0 & 1 & 0 \\ 0 & 0 & 0 & 0 & 0 & 1 \end{pmatrix}.$$

3.1.2 Uncertainty in trajectory prediction

To account for the errors in sensor measurements and the limitations in kinematic modeling, it is necessary to introduce

noise in order to represent the uncertainty in the trajectory prediction process. Filtering algorithms such as the Extended Kalman Filter (EKF) and Unscented Kalman Filter (UKF) (Arulampalam et al., 2002) can be utilized to estimate the uncertainty of the predicted trajectory. In this work, we employ the EKF to estimate the uncertainty of the predicted trajectory, which is described by the covariance matrix $\hat{\boldsymbol{P}}$. The uncertainty of the iterative prediction process of EKF can be expressed as Eq. (5):

$$\hat{\boldsymbol{P}}_{k+1} = \boldsymbol{F}\hat{\boldsymbol{P}}_k\boldsymbol{F}^T + \boldsymbol{Q}_k \tag{5}$$

where $\boldsymbol{F}$ is the coefficient matrix and $\boldsymbol{Q}$ is the process noise matrix.

For the CTRA model, $\boldsymbol{F} = \mathrm{I} + \mathrm{J}\left(\Delta \boldsymbol{X}_{k+1}^1\right)$, $\boldsymbol{Q} = \boldsymbol{G}\boldsymbol{G}^T$, $\boldsymbol{G} = \begin{pmatrix} \frac{1}{6}\sigma_a T_s^3 \cos\left(\theta + 0.5\sigma_w T_s^2\right) \\ \frac{1}{6}\sigma_a T_s^3 \sin\left(\theta + 0.5\sigma_w T_s^2\right) \\ 0.5\sigma_w T_s^2 \\ 0.5\sigma_a T_s^2 \\ \sigma_w T_s \\ \sigma_a T_s \end{pmatrix}$, where $\mathrm{J}(\cdot)$ is the Jacobian matrix; $\boldsymbol{G}$ is the process noise vector; σ_a and σ_w are the measurement noise of a and w, respectively..

For the CA model, $F = A$, $\boldsymbol{Q} = \boldsymbol{B}\omega\omega^T\boldsymbol{B}^T$, $\boldsymbol{B} = \begin{pmatrix} 0.5T_s^2 & 0 \\ 0 & 0.5T_s^2 \\ T_s & 0 \\ 0 & T_s \\ 1 & 0 \\ 0 & 1 \end{pmatrix}$, where ω is the measurement noise vector of a_x and a_y.

3.2 Time-series analysis-based state prediction

In previous studies, when using the vehicle kinematic model to predict the future motion trajectory of the vehicle, it was assumed that the input state sequence of the model was a constant sequence (Lefèvre et al., 2014). This assumption does not match the actual situation. Therefore, the kinematic model only has high accuracy in the short-term prediction of vehicle trajectory.

In this study, inspired by data-driven methods, a time-series analysis module was introduced before trajectory prediction to enable the kinematic model to maintain high prediction accuracy over a longer period. The module leverages historical state sequence of the sideslip vehicle to predict future state sequence, such as acceleration or angular velocity. The predicted state sequence is then employed to replace the constant state sequence for trajectory prediction in the kinematic model, thus enhancing its long-term prediction accuracy. The process of time-series analysis-based future state sequence prediction is depicted in Fig. 3, which encompasses three main steps: Data pre-processing, Calculation of adaptive coefficients, and Prediction of future state sequence.

3.2.1 *Data pre-processing*

Before conducting a time-series analysis on the historical state sequence of the sideslip vehicle, it is necessary to pre-process it, which includes three steps: Gaussian smoothing, Trend sequence extraction, and Trend sequence change feature extraction.

1) Gaussian smoothing: Irregular data in the historical state sequence is smoothed to avoid affecting the subsequent trend sequence extraction.

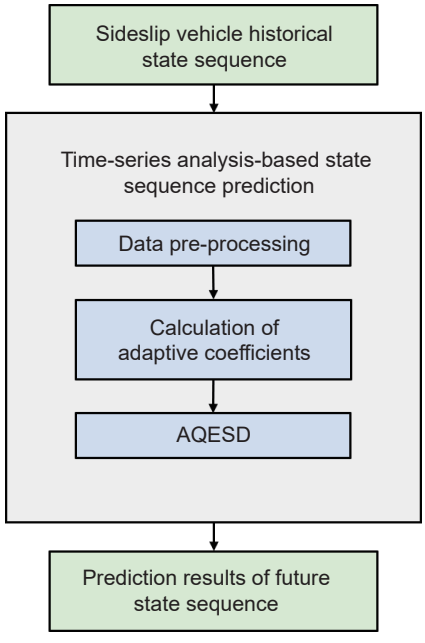

Fig. 3 Process of time-series analysis-based state sequence prediction.

2) Trend sequence extraction: In the process of sideslip, the state of the vehicle is constantly changing, so it is necessary to extract the nearest trend sequence from the observation moment to avoid the negative influence of other invalid sequences on the prediction.

3) Trend sequence change feature extraction: the change feature of trend sequence is expressed using the variance of its slope.

$$ss_{\mathrm{dh}} = \mathrm{diff}\left(ss_{\mathrm{h}}\right) \tag{6}$$

$$ss_{\mathrm{fdh}} = \mathrm{var}\left(ss_{\mathrm{dh}}\right) \tag{7}$$

where ss_{h} is the historical state sequence, ss_{dh} is the extracted trend sequence, $\mathrm{diff}(\cdot)$ denotes the difference operator, $\mathrm{var}(\cdot)$ denotes the variance operator, and ss_{fdh} is the trend sequence change characteristics.

3.2.2 *Adaptive quadratic exponential smoothing with damping*

In this section, we employ the quadratic exponential smoothing (QES) technique of time-series analysis (Gardner, 1985) to acquire knowledge on the historical trend sequence and forecast the future state sequence of sideslip vehicles. To improve the forecasting performance of the QES method, we incorporate a damping coefficient φ into Eq. (10) and propose a set of adaptive calculation methods for the smoothing coefficient α and the damping coefficient φ. The objective of adding φ in the prediction equation is to penalize and restrict excessively rapid changes in prediction values, thereby avoiding excessively large or small prediction values that can lead to poor trajectory prediction results. Moreover, the coefficient can also introduce nonlinear trends into the prediction equation. Consequently, the proposed method is referred to as the Adaptive Quadratic Exponential Smoothing with Damping method. The AQESD method comprises a series of smoothing equations and a prediction equation. The smoothing equations enable online learning of trend sequences, while the prediction equation facilitates the prediction of future state sequences based on the acquired knowledge. The AQESD method is expressed in the following Eqs. (8)–(10):

$$S_t^{(1)} = \alpha\beta_t + (1-\alpha)\, S_{t-1}^{(1)} \tag{8}$$

$$S_t^{(2)} = \alpha S_t^{(1)} + (1-\alpha)\, S_{t-1}^{(2)} \tag{9}$$

$$\hat{\beta}_{t+T_\mathrm{p}} = l_t + r_t T_\mathrm{p}^{\varphi} \tag{10}$$

where Eqs. (8) and (9) are the smoothing equations, and Eq. (10) is the prediction equation. The time step is denoted as t, $S_t^{(1)}$, and $S_t^{(2)}$ are the primary and quadratic exponential smoothing values at time step t, respectively. β_t is the input historical state at time t, $\hat{\beta}_{t+T_\mathrm{p}}$ is the predicted state at time $t+T_\mathrm{p}$, where T_p is the number of prediction steps. $l_t = 2S_t^{(1)} - S_t^{(2)}$ and $r_t = \left(S_t^{(1)} - S_t^{(2)}\right)\alpha/(1-\alpha)$ are the learning parameters. Specifically, l_t represents the level estimate at time t, while r_t represents the trend estimate at time t.

3.2.3 *Calculation of adaptive coefficients*

To achieve better prediction results in the quadratic exponential smoothing method with damping, different smoothing coefficients α and damping coefficients φ need to correspond to different historical state sequences with different variation trends. In this section, we propose a method to adaptively calculate these two parameters (Smoothing coefficient α and Damping coefficient φ) for the CTRA model and CA model under sideslip conditions.

1) Smoothing coefficient α: If α is small (i.e., close to 0), more weight is given to distant past observations. If α is large (i.e., close to 1), more weight is given to recent observations. To achieve better prediction results, an adaptive method is proposed based on the extracted trend sequence change characteristics (ss_fdh) for the CTRA model and CA model under side slip conditions. If ss_fdh is small, indicating that the trend is likely to remain, a smaller α is used. If ss_fdh is large, indicating that the trend is likely to change rapidly, a larger α is used. When ss_fdh is 0, $\alpha = \alpha_\mathrm{min}$ is used, and when ss_fdh is greater than or equal toκ, $\alpha = \alpha_\mathrm{max}$ is used. The adaptive calculation of α is as Eq. (11):

$$\alpha = (\alpha_\mathrm{max} - \alpha_\mathrm{min})\frac{\min(ss_\mathrm{fdh}, \kappa)}{\kappa} + \alpha_\mathrm{min} \tag{11}$$

where $\min(\cdot)$ is the minimum operator, κ is the trend sequence change characteristic threshold, which is related to the sequence type and is usually obtained through testing. $0 < \alpha_\mathrm{min} < \alpha_\mathrm{max} < 1$, with α_max typically set to 0.9 and α_min typically set to 0.3.

2) Damping coefficient φ: It is assumed that the driver will decelerate the sideslip vehicle, causing the centrifugal force to decrease during the sideslip process due to the decrease in speed and increase in the trajectory radius, as depicted by the green vehicle in Fig. 2. This reduces the sideslip tendency of the vehicle, with the limit of this tendency being when the centrifugal force disappears and the vehicle returns to smooth operation. Once the vehicle regains smoothness, the body no longer rotates when the adhesion force provides all the braking force. The expressions for states a and w are as Eqs. (12) and (13):

$$a_\mathrm{lim} = -\mu g \tag{12}$$

$$w_\mathrm{lim} = 0 \tag{13}$$

where subscript lim presents the limiting state and g is the acceleration of gravity. μ is the road adhesion coefficient, which can be provided by an adhesion coefficient estimation system (Liu et al., 1996).

For states a_x and a_y, the limits are as Eqs. (14) and (15):

$$a_{x\mathrm{lim}} = -\mu g\cos(\lambda\theta_\mathrm{s}) \tag{14}$$

$$a_{y\mathrm{lim}} = -\mu g\sin(\lambda\theta_\mathrm{s}) \tag{15}$$

For lane change conditions,$\lambda = -1.5$ and θ_s is the maximum rotation angle θ during the first turn of the vehicle during lane change. For curve road conditions, $\lambda = 2$ and θ_s is the rotation angle θ of the vehicle when the sideslip is recognized. The setting for λ is determined based on tuning experience.

According to Eq. (10), φ is calculated as Eq. (16):

$$\varphi = \log\left(\frac{\mathrm{lim}_t - l_t}{r_t}\right)/\log T_\mathrm{p} \tag{16}$$

where lim_t is the limiting estimate of the predicted state (i.e., a_lim or w_lim, etc.) at moment t.

3.3 Interacting multiple model

As there is no single model that can fully describe the vehicle's motion state in all scenarios, fusing the prediction results of multiple models to describe the future trajectory of a vehicle is an effective method that can significantly improve the accuracy of the trajectory prediction results of sideslip vehicles. The IMM algorithm (Xie et al., 2017) has the advantage of combining multiple models and being able to adaptively identify and switch between models. Therefore, this study proposes an IMM-based multi-physics model fusion method, TSIMMSTP, for predicting the trajectory of sideslip vehicles.

The IMM method is illustrated in Fig. 4 and consists of four main modules, which are Input Interaction and Mixing, Prediction by Model, Model Probability Update, and Fusion of Prediction. The mean and covariance of the i' model at time step k are represented by $\hat{X}_k^i$ and $\hat{P}_k^i$, respectively. $\hat{X}_k^{mi}$ and $\hat{P}_k^{mi}$ are the mean and covariance of the i'th model at time step k after input interaction and mixing, respectively. The vector of weight coefficients of the two models at prediction moment k is denoted by u_k, while u_k^m represents the vector of weight coefficients of the two models at prediction moment k after input interaction and mixing. The mean, variance, and weight coefficient vectors after the one-step prediction are represented by $\hat{X}_{k+1}$, $\hat{P}_{k+1}$, and u_{k+1}, respectively.

In this study, the predictions of the CTRA model (M^1) and CA model (M^2) are fused by IMM. As a result, the model set (M) of this system consists of discrete models and can be expressed as Eq. (17):

$$M = \left\{M^1, M^2\right\} \tag{17}$$

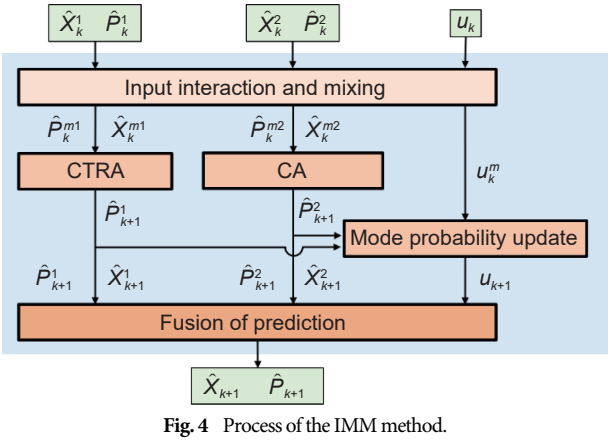

Fig. 4 Process of the IMM method.

In this dynamic system, the prediction of the model M^i interacts according to the change of $\boldsymbol{u}_k$, where $\boldsymbol{u}_k = \left(u_k^1, u_k^2\right)^T$ and $u_k^i = p\left(M_k^i\right)$ represents the probability that model i is used for fusion at moment k, where $i = 1, 2$. The system is a Markov switching system with model transfer probability expressed as Eq. (18):

$$p_{ij} = p\left(M_k^j | M_{k-1}^i\right) \tag{18}$$

1) Input interaction and mixing

The input interaction process, which is based on the dynamically changing weight coefficients and model transfer probabilities of each model, can be expressed as Eqs. (19) and (20):

$$\bar{c}_j = \sum_{i=1,2} p_{ij} u_k^i \tag{19}$$

$$u_k^{i|j} = \frac{1}{\bar{c}_j} p_{ij} u_k^i \tag{20}$$

where $\bar{c}_j$ is the normalization factor. The mean and covariance of each model after Gaussian mixing can be expressed as Eq. (21):

$$\hat{X}_k^{mj} = \sum_{i=1,2} u_k^{i|j} \hat{X}_k^i \tag{21}$$

$$\hat{P}_k^{mj} = \sum_{i=1,2} u_k^{i|j} \left[\hat{P}_k^i + \left(\hat{X}_k^i - \hat{X}_k^{mj}\right)\left(\hat{X}_k^i - \hat{X}_k^{mj}\right)^T\right] \tag{22}$$

2) Prediction by model

The mean and covariance after mixing are fed into their corresponding prediction models for the next step of mean and variance prediction, respectively. The prediction process for each model can be expressed as Eq. (23):

$$\left(\hat{X}_{k+1}^i, \hat{P}_{k+1}^i\right) = \mathrm{Pred}_i\left(\hat{X}_k^{mi}, \hat{P}_k^{mi}\right) \tag{23}$$

where $\mathrm{Pred}_i(\cdot)$ denotes prediction model i.

3) Model probability update

The model probabilities of the predicted outcomes are updated using the maximum likelihood method. In this study, the designed likelihood function is expressed as Eq. (24):

$$\Lambda_{k+1}^i = \frac{1}{\left(sa_{ce}^i\right)^2 + \left(sb_{ce}^i\right)^2} \tag{24}$$

where $sa_{ce}^i = \mathrm{maxeig}\left(\hat{P}_{xy}^i\right)$ is the maximum eigenvalue of the covariance matrix $\hat{P}_{xy}^i$ and $sb_{ce}^i = \mathrm{mineig}\left(\hat{P}_{xy}^i\right)$ is the minimum eigenvalue of $\hat{P}_{xy}^i$. $\hat{P}_{xy}^i$ is the covariance matrix associated with x and y of model i, and the operators $\mathrm{maxeig}(\cdot)$ and $\mathrm{mineig}(\cdot)$ respectively represent the maximum and minimum eigenvalues.

The probability after each model update is Eq. (25):

$$u_{k+1}^i = \frac{1}{c} \Lambda_{k+1}^i \bar{c}_i \tag{25}$$

where $c = \sum_{i=1,2} \Lambda_{k+1}^i \bar{c}_i$.

4) Fusion of prediction

Finally, utilizing the updated model probabilities, the predictions of each model are fused to obtain the mean and variance after fusion, expressed as Eqs. (26) and (27):

$$\hat{X}_{k+1} = \sum_{i=1,2} u_{k+1}^i \hat{X}_{k+1}^i \tag{26}$$

$$P_{k+1} = \sum_{i=1,2} u_{k+1}^i \left(\hat{P}_{k+1}^i + \left(\hat{X}_{k+1}^i - \hat{X}_{k+1}\right)\left(\hat{X}_{k+1}^i - \hat{X}_{k+1}\right)^T\right) \tag{27}$$

4 Simulation

As reported in Xiang et al. (2022), dangerous sideslip of vehicles on highways mainly occurs in two scenarios: lane change and curve road scenarios. In this section, the proposed vehicle sideslip trajectory prediction method will be employed in these scenarios. To evaluate the proposed method, different conditions are designed for these scenarios. Various sideslip trajectory prediction methods are applied to these conditions, and the prediction results are compared and analyzed.

4.1 Simulation scheme design

Using the simulation software CARSIM, simulation scenarios are designed to compare and analyze the performance of different sideslip trajectory prediction methods. To demonstrate the applicability of the proposed method to different vehicles, four different vehicle models, including hatchback, sedan, etc., in CARSIM are selected. According to the speed limit requirements of Chinese highways, we have set the initial velocities of these vehicles to be 90, 100, 110, and 120 km/h, respectively. For the lane change scenario, a fifth-order polynomial method is used to generate the trajectory, and the lane change time is set to 2 or 3 s for emergency lane change (Shiller and Sundar, 1998). For the curve road scenario, according to highway road design standards, the radius is set to 300 or 650 m. In real-world highways, speed limits are usually imposed on curves with smaller radii. Therefore, for the scenario with a radius of 300 m, only two initial velocities, 90 km/h and 100 km/h, are considered. A total of 56 sub-scenarios are designed, as shown in Table 1. The duration of the sideslip trajectory in all sub-scenarios is between 3 and 5 s, and the prediction time is from the beginning of the sideslip to the end.

4.2 Statistical analysis of sideslip trajectory prediction

The performance of six different methods, namely CA, CTRA, and CA model with time-series analysis (TSCA), CTRA model with time-series analysis (TSCTRA), Weight Function (WF) method (Houenou et al., 2013), and TSIMMSTP, for predicting vehicle sideslip trajectories were evaluated in all the 56 sub-scenarios using Final Displacement Error (FDE) and Average Displacement Error (ADE) metrics (Liu et al., 2022). The

Table 1 Simulation scenarios design

Scenario	Type of vehicle				Initial velocity (km/h)			
	A class hatchback	B class hatchback	C class hatchback	D class sedan	90	100	110	120
Lane change 2 s	√	√	√	√	√	√	√	√
Lane change 3 s	√	√	√	√	√	√	√	√
Curve road R300	√	√	√	√	√	√	—	—
Curve road R650	√	√	√	√	√	√	√	√

evaluation was performed in the time domain from 1 s until the end of the sideslip. The results are presented in Table 2. It can be observed that all five methods achieve high prediction accuracy within the first second in different driving scenarios. However, as the prediction time increases, the prediction errors of CA and CTRA increase rapidly, while those of TSCA, TSCTRA, and WF increase at a slower rate, and the prediction error of TSIMMSTP increases the slowest. At the end of the prediction, the TSIMMSTP achieves 3–6 times improvement for FDE and 2.5–4 times improvement for ADE performance indicators compared to CA and CTRA, respectively. This indicates that incorporating a time-series analysis module and an IMM-based fusion model into the vehicle's trajectory prediction system enables more accurate prediction of the future position of sliding vehicles. This allows the ego vehicle, located in an adjacent lane to the sliding vehicle, to make more informed decisions and plans, such as appropriate braking or lane changing, thereby reducing the probability of collision with the sliding vehicle.

4.3 Case study of the sideslip trajectory prediction

This section presents a detailed analysis and comparison of the TSIMMSTP method for providing high-precision long-term predictions of vehicle sideslip trajectories. The advantages of TSIMMSTP over the WF method, as shown in Table 2, have already been established, and thus the WF method was not considered for subsequent analysis. Initially, we showcased the superiority of the proposed AQESD method over QES and constant sequences (without time-series analysis) through a case study. Following that, we conducted a comparative analysis of the predictive performance of CA, CTRA, TSCA, and TSCTRA, thereby highlighting the benefits of the TS module. Finally, we performed a detailed comparison of the predictive performance of three models, namely, TSCA, TSCTRA, and TSIMMSTP, to demonstrate the advantages of introducing the IMM module.

4.3.1 *Case study for AQESD*

Fig. 5 presents a comparison of different time-series analysis methods for predicting the state sequences a_x and a_y in a lane-changing sub-scenario using the CA model. Real_seq represents the true sequence to be predicted, His_seq is the historical sequence, AQESD is the prediction result of AQESD, and QES ($\alpha = 0.3$) and QES ($\alpha = 0.9$) are the prediction results of QES with smoothing coefficients of 0.3 and 0.9, respectively. Con_seq is the constant sequence. Fig. 5b compares the predicted future sequences of a_y, where the trend of the historical sequence of a_y is relatively stable. In this case, both AQESD and QES can predict the future trend of the a_y sequence, with little difference between them, while the sequence predicted by AQESD is superior to QES, and constant sequences cannot reflect the future trend of a_y. Fig. 5a compares the predicted future sequences of a_x, where the

Table 2 Evaluation and comparison of prediction results in terms of FDE/ADE (Unit: m)

Method	Scenario: Lane change 2 s				
	1 s	2 s	3 s	4 s	End
CA	0.14/0.04	0.92/0.27	2.65/0.77	3.81/1.11	5.61/1.62
CTRA	0.11/0.04	0.65/0.20	1.74/0.54	2.41/0.75	3.41/1.06
TSCA	0.1/0.04	0.37/0.13	0.82/0.31	0.95/0.37	1.18/0.52
TSCTRA	0.1/0.04	0.36/0.13	0.98/0.34	1.41/0.42	2.12/0.62
WF	0.1/0.04	0.35/0.13	0.73/0.28	0.90/0.35	1.15/0.43
TSIMMSTP	0.1/0.04	0.35/0.13	0.62/0.25	0.82/0.31	1.03/0.40
Method	Scenario: Lane change 3 s				
	1 s	2 s	3 s	4 s	End
CA	0.09/0.03	0.66/0.19	1.95/0.56	4.16/1.19	7.80/2.23
CTRA	0.07/0.03	0.51/0.15	1.46/0.43	2.97/0.88	5.31/1.59
TSCA	0.06/0.02	0.34/0.11	0.79/0.29	1.20/0.45	1.56/0.66
TSCTRA	0.06/0.02	0.31/0.10	0.77/0.27	1.67/0.50	3.43/0.93
WF	0.06/0.02	0.30/0.10	0.73/0.25	1.16/0.43	1.53/0.63
TSIMMSTP	0.06/0.02	0.30/0.10	0.72/0.24	1.12/0.42	1.51/0.62
Method	Scenario: Curve road R300				
	1 s	2 s	3 s	4 s	End
CA	0.12/0.04	1.11/0.30	3.56/0.98	5.00/1.38	6.01/1.65
CTRA	0.09/0.03	0.86/0.23	2.68/0.74	3.73/1.04	4.40/1.23
TSCA	0.08/0.03	0.52/0.16	1.10/0.34	1.35/0.50	1.48/0.52
TSCTRA	0.07/0.03	0.50/0.15	1.32/0.36	1.72/0.55	2.39/0.63
WF	0.07/0.03	0.45/0.15	0.98/0.32	1.30/0.45	1.38/0.49
TSIMMSTP	0.07/0.03	0.45/0.15	0.89/0.31	1.20/0.40	1.28/0.44
Method	Scenario: Curve road R650				
	1 s	2 s	3 s	4 s	End
CA	0.05/0.01	0.47/0.12	1.43/0.40	1.93/0.54	2.06/0.58
CTRA	0.05/0.01	0.41/0.11	1.21/0.34	1.61/0.46	1.71/0.49
TSCA	0.02/0.01	0.19/0.05	0.46/0.14	0.56/0.18	0.58/0.19
TSCTRA	0.02/0.01	0.15/0.04	0.54/0.15	0.78/0.19	0.82/0.20
WF	0.02/0.01	0.15/0.04	0.41/0.13	0.52/0.16	0.54/0.17
TSIMMSTP	0.02/0.01	0.15/0.04	0.39/0.12	0.50/0.15	0.52/0.16

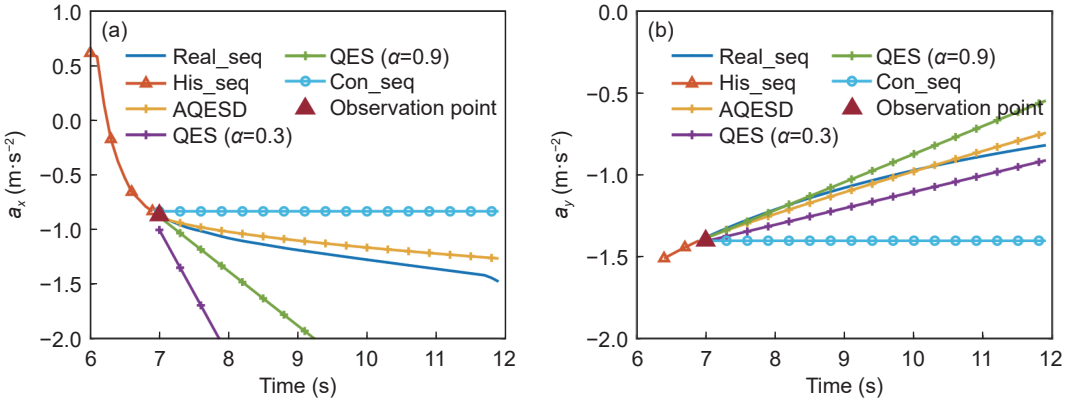

Fig. 5 Comparison of state sequence prediction results.

trend of the historical sequence of a_x is not stable, with a sharp decline followed by a gradual slowing down. In this case, there is a large difference between the prediction results of AQESD and QES for a_x. In QES, if the smoothing coefficient is small, such as 0.3, the predicted sequence trend is consistent with the trend of distant historical data, while if the smoothing coefficient is large, such as 0.9, the predicted sequence trend is consistent with the trend of recent historical data. When the smoothing coefficient is large, the predicted results to be closer to the true results, indicating that a larger smoothing coefficient should be used when the trend of the historical sequence is unstable. However, in QES, since there is no punishment or limitation for the changes and maximum values of the predicted sequence, the predicted sequence quickly deviates from the true sequence. In AQESD, taking $\kappa = 0.5$ and calculating the smoothing coefficient based on Eq. (11) also gives a value of 0.9, but a damping coefficient φ is added to AQESD, which is calculated as 0.55 based on Eq. (16). This punishes the growth of the predicted future sequence of a_x and limits its maximum value, ultimately allowing AQESD to produce predictions that are close to the true results for a_x. The constant sequence also cannot reflect the future trend of a_x. For the CTRA model, AQESD plays the same role as described above, and thus, we will not repeat it here.

The results above indicate that under the condition of a stable trend in the historical state sequence, QES can effectively predict the changing trend of future state sequences. However, when the trend in the historical state sequence is unstable, the predictive performance of QES for future state sequences deteriorates. This issue can be effectively addressed by utilizing the proposed AQESD. It is worth noting that a constant sequence cannot reflect the future trend of the state. Therefore, replacing the input of the kinematic model with the predictive results of AQESD for state sequences will be beneficial for improving the long-term prediction accuracy of the kinematic model for the trajectory of the sideslip vehicle.

4.3.2 *Case study for TSIMMSTP*

In Fig. 6, the red car is the observed sideslip vehicle. Figs. 6a and

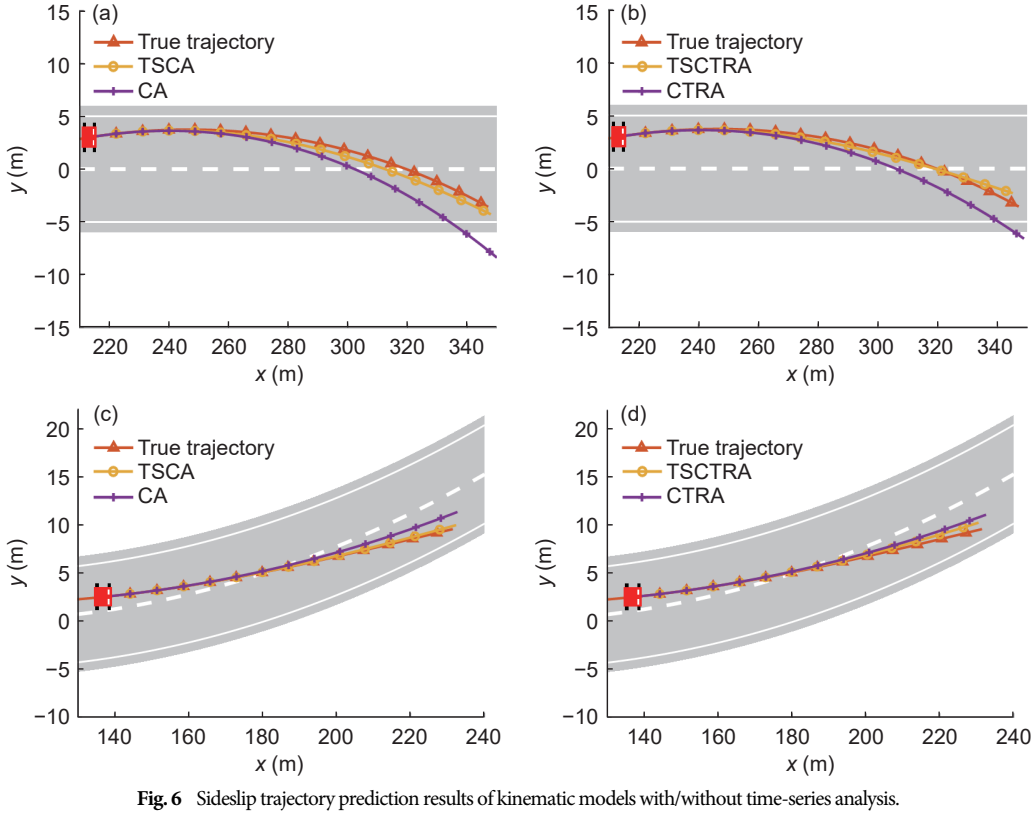

Fig. 6 Sideslip trajectory prediction results of kinematic models with/without time-series analysis.

6b show the comparison of the predicted sideslip trajectories between the TSCA and CA models, and between the TSCTRA and CTRA models, respectively, in the lane change scenario of 3 s. Figs. 6c and 6d show the comparison of the predicted sideslip trajectories between the TSCA and CA models, and between the TSCTRA and CTRA models, respectively, in the curve road scenario of R650. Figs. 7a–7d depict the corresponding comparison of the prediction errors, where the prediction errors are measured using the direct Euclidean distance between the real trajectory and the predicted trajectory. The results show that the effect of introducing a time-series analysis module on the prediction error within 1 s is not significant for both the CTRA and CA models. However, after 1 s, the prediction error of the physical model without a time-series analysis module increases rapidly, while that of the model with a time-series analysis module increases slowly. At the end of the prediction, in the lane change sub-scenario, the final errors of TSCA and TSCTRA are 5.6 and 1.3 m smaller than those of CA and CTRA, respectively. In the curve road sub-scenario, the final errors of TSCA and TSCTRA are 1.3 and 0.8 m smaller than those of CA and CTRA, respectively. This indicates that the introduction of the TS module can effectively enhance the accuracy of the ego vehicle's prediction of the trajectory of the sliding vehicle, both in straight and curved road scenarios. The ego vehicle can more accurately determine when and where the sliding vehicle will slide out of the lane, and consequently take timely safety measures to avoid collisions with the sliding vehicle.

Fig. 8 shows the comparison of the predicted sideslip trajectory and uncertainty region of the TSCTRA, TSCA, and TSIMMSTP. Figs. 9 and 10 show the corresponding prediction error comparison and model probability transition. It can be observed that at the beginning, the prediction error and uncertainty of the TSCTRA model are small, and its probability is close to 1. As a result, the fused prediction error grows consistently with the TSCTRA model's prediction error. As time progresses, the prediction error and uncertainty of the TSCTRA model become

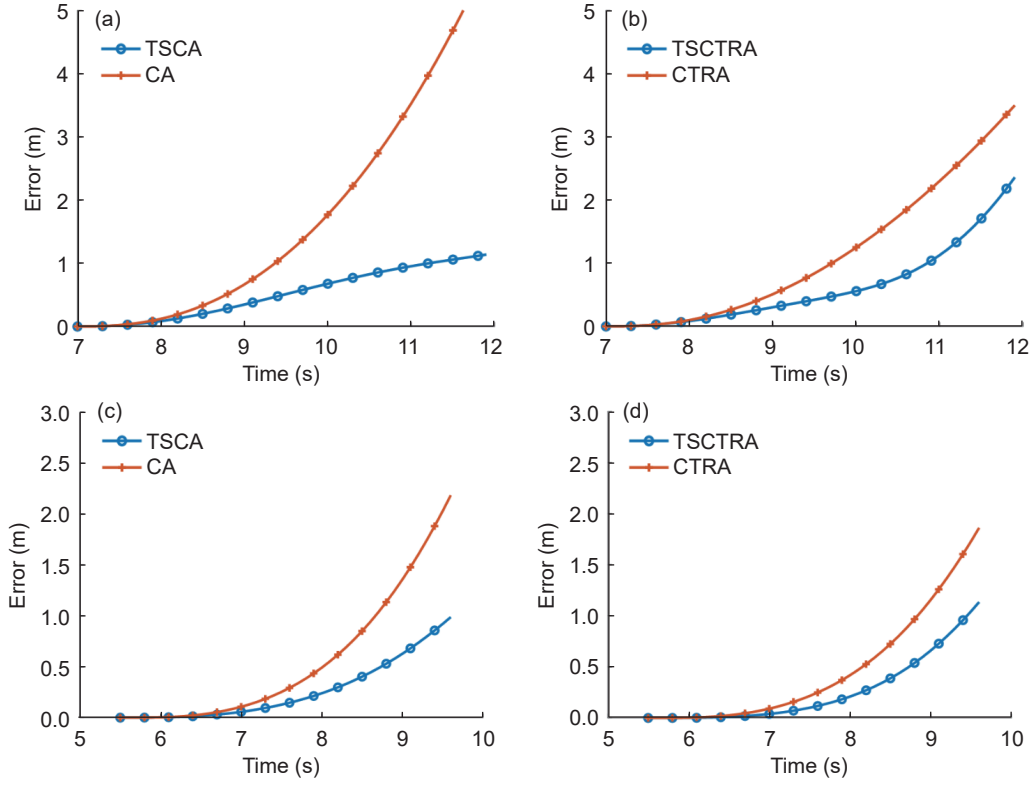

Fig. 7 Sideslip trajectory prediction errors of kinematic models with/without time-series analysis.

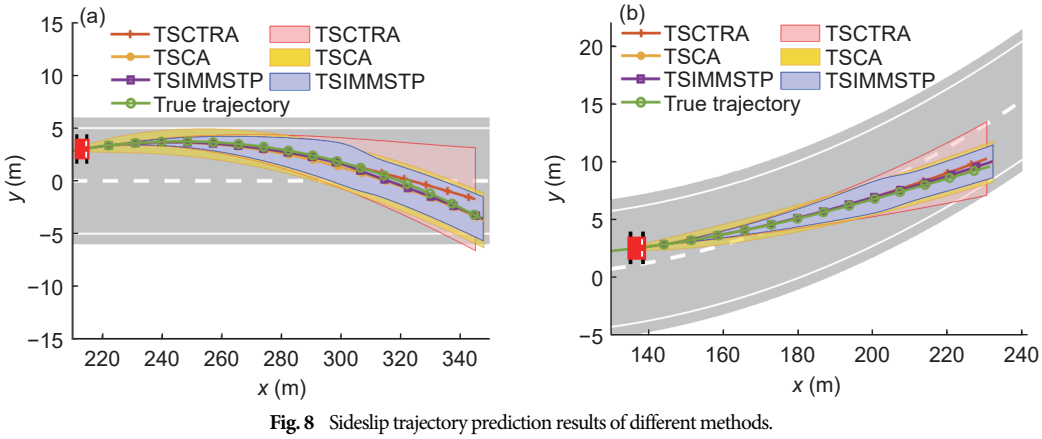

Fig. 8 Sideslip trajectory prediction results of different methods.

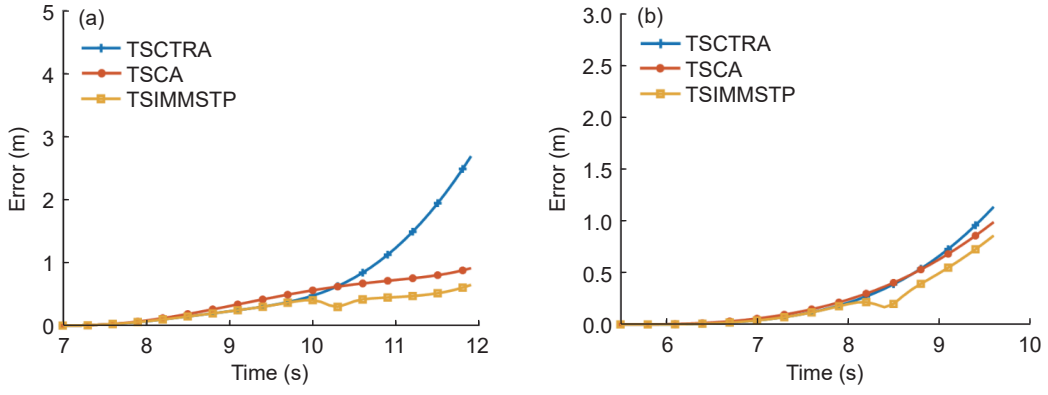

Fig. 9 Sideslip trajectory prediction errors of different methods.

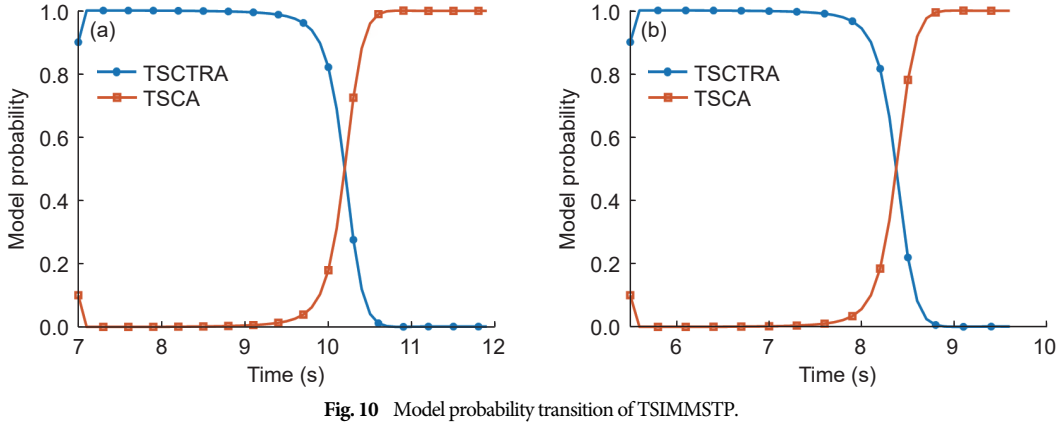

Fig. 10 Model probability transition of TSIMMSTP.

larger than that of the TSCA model. At this point, the probability of the TSCA model approaches 1, and the fused prediction error transitions from growing consistently with the TSCTRA model's prediction error to growing consistently with the TSCA model's prediction error trend. Since the fused prediction error is smaller than the TSCA model's prediction error before the transition occurs, the fused prediction error is the smallest at the end of the prediction. At the end of the prediction, the final prediction error of TSIMMSTP is less than 1 m in both sub-scenarios.

Table 3 compares the variation of prediction uncertainty before and after the fusion of TSCTRA and TSCA models using IMM in the two different scenarios, where uncertainty is represented by the average three times standard deviation in the prediction horizon. Table 3 and Fig. 8 show that the uncertainty after fusion is smaller than before, indicating that TSIMMSTP not only improves the accuracy of trajectory prediction but also reduces its uncertainty. The aforementioned findings illustrate that the integration of both the time-series analysis module and the trajectory fusion module into the vehicle's trajectory prediction system not only facilitates a more precise estimation of the sliding vehicle's position but also improves the dependability of the prediction outcomes. Consequently, the ego vehicle can operate within a broader feasible driving area and employ more flexible obstacle avoidance strategies, making it easier to avoid collisions with the sliding vehicle.

Table 3 Comparison of prediction uncertainty using three times standard deviation (Unit: m)

Case	Method	1 s	2 s	3 s	4 s	End
Lane change	TSCA	0.72	1.06	1.32	1.54	1.72
	TSCTRA	0.14	0.46	0.87	1.37	1.94
	TSIMMSTP	0.13	0.45	0.86	1.17	1.39
Curve road	TSCA	0.53	0.79	0.98	1.14	1.17
	TSCTRA	0.12	0.39	0.74	1.17	1.26
	TSIMMSTP	0.11	0.38	0.72	0.92	0.95

5 Conclusions

In this study, we proposed a novel trajectory prediction method for vehicle sideslip trajectories based on time-series analysis and multi-physical model fusion. The method enables high-precision and long-term prediction of vehicle sideslip trajectories.

This study draws the following conclusions. First, the proposed AQESD method in the time-series analysis module can predict the trend of future state sequences and provide more accurate inputs for physical models, thus improving the long-term prediction accuracy of kinematic-based methods. Second, the proposed TSIMMSTP can adaptively switch between kinematic models and effectively fuse several sideslip trajectory prediction results of kinematic models, further improving the long-term prediction accuracy of kinematic-based methods.

In the future, we plan to integrate this algorithm into the decision and control module and validate the effectiveness of this method through hardware-in-the-loop or real vehicle experiments.

Acknowledgements

This research was supported by the National Natural Science Foundation of China (Grant No. 51975310).

Declaration of competing interest

The authors have no competing interests to declare that are relevant to the content of this article.

References

Alahi, A., Goel, K., Ramanathan, V., Robicquet, A., Li, F. F., Savarese, S., 2016. Social LSTM: Human trajectory prediction in crowded spaces. In: 2016 IEEE Conference on Computer Vision and Pattern Recognition (CVPR), 961–971.

Ammoun, S., Nashashibi, F., 2009. Real time trajectory prediction for collision risk estimation between vehicles. In: 2009 IEEE 5th International Conference on Intelligent Computer Communication and Processing, 417–422.

Arulampalam, M. S., Maskell, S., Gordon, N., Clapp, T., 2002. A tutorial on particle filters for online nonlinear/non-Gaussian Bayesian tracking. IEEE Trans Signal Process, 50, 174–188.

Bahari, M., Saadatnejad, S., Rahimi, A., Shaverdikondori, M., Shahidzadeh, A. H., Moosavi-Dezfooli, S. M. *et al*., 2022. Vehicle trajectory prediction works, but not everywhere. In: 2022 IEEE/CVF Conference on Computer Vision and Pattern Recognition (CVPR), 17102–17112.

Deo, N., Trivedi, M. M., 2018. Convolutional social pooling for vehicle trajectory prediction. In: 2018 IEEE/CVF Conference on Computer Vision and Pattern Recognition Workshops (CVPRW), 1549–15498.

Eskandarian, A., Wu, C., Sun, C., 2021. Research advances and challenges of autonomous and connected ground vehicles. IEEE Trans Intell Transp Syst, 22, 683–711.

Fang, L., Jiang, Q., Shi, J., Zhou, B., 2020. TPNet: trajectory proposal network for motion prediction. In: 2020 IEEE/CVF Conference on Computer Vision and Pattern Recognition (CVPR), 6796–6805.

Gardner, E. S., 1985. Exponential smoothing: The state of the art. J Forecast, 4, 1–28.

Ghorai, P., Eskandarian, A., Kim, Y. K., Mehr, G., 2022. State estimation and motion prediction of vehicles and vulnerable road users for cooperative autonomous driving: A survey. IEEE Trans Intell Transp Syst, 23, 16983–17002.

Gulzar, M., Muhammad, Y., Muhammad, N., 2021. A survey on motion prediction of pedestrians and vehicles for autonomous driving. IEEE Access, 9, 137957–137969.

Houenou, A., Bonnifait, P., Cherfaoui, V., Wen, Y., 2013. Vehicle trajectory prediction based on motion model and maneuver recognition. In: 2013 IEEE/RSJ International Conference on Intelligent Robots and Systems (IROS 2013), 4363–4369.

Huang, Y., Du, J., Yang, Z., Zhou, Z., Zhang, L., Chen, H., 2022. A survey on trajectory-prediction methods for autonomous driving. IEEE Trans Intell Veh, 7, 652–674.

Izquierdo, R., Quintanar, Á., Llorca, D. F., Daza, I. G., Hernández, N., Parra, I., *et al*., 2023. Vehicle trajectory prediction on highways using bird eye view representations and deep learning. Appl Intell, 53, 8370–8388.

Kim, W., Kang, C. M., Son, Y. S., Lee, S. H., Chung, C. C., 2018. Vehicle path prediction using yaw acceleration for adaptive cruise control. IEEE Trans Intell Transp Syst, 19, 3818–3829.

Lefèvre, S., Vasquez, D., Laugier, C., 2014. A survey on motion prediction and risk assessment for intelligent vehicles. ROBOMECH J, 1, 1–14.

Liang, M., Yang, B., Hu, R., Chen, Y., Liao, R., Feng, S., *et al*., 2020. Learning lane graph representations for motion forecasting. Computer Vision – ECCV 2020. Cham: Springer International Publishing, 541–556.

Liu, C. S., Peng, H., 1996. Road friction coefficient estimation for vehicle path prediction. Veh Syst Dyn, 25, 413–425.

Liu, J., Luo, Y., Zhong, Z., Li, K., Huang, H., Xiong, H., 2022. A probabilistic architecture of long-term vehicle trajectory prediction for autonomous driving. Engineering, 19, 228–239.

Messaoud, K., Yahiaoui, I., Verroust-Blondet, A., Nashashibi, F., 2019. Non-local social pooling for vehicle trajectory prediction. In: 2019 IEEE Intelligent Vehicles Symposium (IV), 975–980.

Messaoud, K., Yahiaoui, I., Verroust-Blondet, A., Nashashibi, F., 2021. Attention based vehicle trajectory prediction. IEEE Trans Intell Veh, 6, 175–185.

Mozaffari, S., Al-Jarrah, O. Y., Dianati, M., Jennings, P., Mouzakitis, A., 2022. Deep learning-based vehicle behavior prediction for autonomous driving applications: A review. IEEE Trans Intell Transp Syst, 23, 33–47.

Park, J. H., Tai, Y. W., 2015. A simulation based method for vehicle motion prediction. Comput Vis Image Underst, 136, 79–91.

Schreier, M., Willert, V., Adamy, J., 2016. An integrated approach to maneuver-based trajectory prediction and criticality assessment in arbitrary road environments. IEEE Trans Intell Transp Syst, 17, 2751–2766.

Schubert, R., Richter, E., Wanielik, G., 2008. Comparison and evaluation of advanced motion models for vehicle tracking. In: 2008 11th International Conference on Information Fusion, 1–6.

Shiller, Z., Sundar, S., 1998. Emergency lane-change maneuvers of autonomous vehicles. J Dyn Syst Meas Contr, 120, 37–44.

Song, H., Luan, D., Ding, W., Wang, M. Y., Chen, Q., 2022. Learning to Predict Vehicle Trajectories with Model-based Planning. In: Proceedings of the 5th Conference on Robot Learning, 1035–1045.

Wissing, C., Nattermann, T., Glander, K. H., Bertram, T., 2018. Trajectory prediction for safety critical maneuvers in automated highway driving. In: 2018 21st International Conference on Intelligent Transportation Systems (ITSC), 131–136.

Xiang, Y., He, Y., Luo, Y., Bu, D., Kong, W., Chen, J., 2022. Recognition model of sideslip of surrounding vehicles based on perception information of driverless vehicle. IEEE Intell Syst, 37, 79–91.

Xie, G., Gao, H., Qian, L., Huang, B., Li, K., Wang, J., 2018. Vehicle trajectory prediction by integrating physics- and maneuver-based approaches using interactive multiple models. IEEE Trans Ind Electron, 65, 5999–6008.

Yao, H., Li, Q., Li, X., 2022. Trajectory prediction dimensionality reduction for low-cost connected automated vehicle systems. Transp Res Part D Transp Environ, 111, 103439.

Yao, H., Li, X., Yang, X., 2023. Physics-aware learning-based vehicle trajectory prediction of congested traffic in a connected vehicle environment. IEEE Trans Veh Technol, 72, 102–112.

Zhang, Q., Hu, S., Sun, J., Chen, Q. A., Mao, Z. M., 2022. On adversarial robustness of trajectory prediction for autonomous vehicles. https://arxiv.org/abs/2201.05057

Lipeng Cao received the B.S. and M.S. degrees in automotive engineering from Chongqing University, Chongqing, China, in 2017 and 2020, respectively, where he is currently pursuing the Ph.D. degree with the College of Mechanical and Vehicle Engineering. He is also a joint student of the State Key Laboratory of Automotive Safety and Energy, Tsinghua University, Beijing, China. His research interests include the safety of the intended functionality (SOTIF) and vehicle localization and control technology.

Yugong Luo (Member, IEEE) received the B. Tech. and M.S. degrees from Chongqing University, Chongqing, China, in 1996 and 1999, respectively, and the Ph.D. degree from Tsinghua University, Beijing, China, in 2003. He is currently a Professor with the School of Vehicle and Mobility, Tsinghua University. His research interests include intelligent connected electric vehicle dynamics and control and vehicle noise control.

Yongsheng Wang earned the Ph.D. degree in vehicle engineering from the China Agricultural University, Beijing, China, in 2022. He is currently a Postdoctoral Researcher with the School of Vehicle and Mobility, Tsinghua University, Beijing, China. His research interests include vehicle dynamics and control and the safety of the intended functionality of vehicle localization systems.

Jian Chen received the B.Tech. degree from Hefei University of Technology, China, in 1993. He is currently pursuing the Ph.D. degree in Tsinghua University, Beijing, China. His main interests include artificial intelligence, focusing on theoretical and practical aspects of argumentation-based reasoning.

Yansong He received the B.Tech., M.S., and Ph.D. degrees from Chongqing University, Chongqing, China, in 1990, 1993, and 2003, respectively. He is currently a Professor with the College of Mechanical and Vehicle Engineering, Chongqing University. His research interests include autonomous vehicles, vehicle dynamics, and vehicle noise control.